DEVELOPMENT OF A HYBRID MOBILE ROBOT NAVIGATION SYSTEM FOR INDUSTRIAL APPLICATIONS

IVAN ZAJACKO[1], VLADIMIR BENKO[1], PAVOL BOZEK[1]

[1]University of Zilina, Faculty of Mechanical Engineering, Zilina, Slovakia

DOI: 10.17973/MMSJ.2026_06_2026119

pavol.bozek@fstroj.uniza.sk

This article addresses the problem of constructing an accurate and reliable navigation system for autonomous mobile robots (MR) operating in environments where Global Navigation Satellite System (GNSS) signals are unavailable. A hybrid approach is proposed, combining data from odometry, an electronic compass, and an active ultrasonic beacon system. Based on the technical specification for the development of a heavy mobile robot (mass 200 kg with payload), the selection of sensors and control algorithms is justified. Mathematical modeling includes a trilateration method with temperature compensation of the speed of sound and data filtering based on an Extended Kalman Filter (EKF). Experimental results confirm the possibility of achieving positioning accuracy of ±10 cm in steady-state operation: the coordinate determination error did not exceed 12 cm in dynamic mode and 8 cm in static mode. Initial transient errors during EKF convergence (up to 2 m) are effectively suppressed within 3–5 seconds of system operation.

KEYWORDS

mobile robot, navigation, trilateration, ultrasonic beacons, odometry, electronic compass, Kalman filter, control system

1 INTRODUCTION

Autonomous mobile robots are widely used in logistics, infrastructure inspection, and industrial automation. A key challenge in developing such systems is ensuring reliable navigation and control under environmental uncertainty. The development of control systems for robots of significant mass is particularly relevant, as the inertial properties of the object impose strict requirements on the response time of control loops and positioning accuracy [Galieva 2023, Kuric 2022].

In industrial premises or enclosed facilities, GPS/GLONASS signals are often unavailable or have unacceptable errors. Existing solutions based on laser scanners (SLAM) offer high accuracy but require significant computational resources and are sensitive to dust and lighting conditions [Vlasov 2017, Nikitin 2025, Bozek 2016]. An alternative is beacon-based systems and inertial navigation, which can provide sufficient accuracy at a lower cost [Detkova 2023].

The aim of this work is to develop a hybrid navigation system for a mobile robot capable of autonomously moving to a specified target, determining its coordinates, and avoiding obstacles, while meeting the requirements of the technical specification for a robot with a payload capacity of 100 kg [Ivanov 2022].

Scientific novelty of this work lies in the following:

A. Adaptation of ultrasonic trilateration for inertial objects: For the first time, a method of temperature compensation of the speed of sound is proposed in the control loop of a heavy mobile robot (mass 200 kg), where inertial properties require high positioning accuracy to prevent emergency situations.
B. Hybrid architecture with Kalman filtering: A measurement scheme is developed that combines odometry data (high frequency) and ultrasonic beacons (absolute accuracy) using an Extended Kalman Filter to compensate for the drift of inertial sensors.
C. Integration with an ontological model (perspective): The work outlines a direction for implementing semantic navigation, which distinguishes it from purely metric approaches (SLAM).

2 LITERATURE REVIEW AND ANALYSIS OF EXISTING SOLUTIONS

The problem of local robot orientation is discussed in detail in the monograph by Vlasov S.M. et al. [Vlasov 2017], where navigation methods are classified: odometry, beacon systems, computer vision, and laser localization. The authors note that odometry is prone to error accumulation due to wheel slippage but remains indispensable for short-term velocity tracking [Leiva 2023, Zidek 2024].

Beacon systems are effective for correcting global coordinates. Zatekin D.V. proposed a positioning system based on active ultrasonic beacons for educational laboratories. This method provides accuracy on the order of 10 cm when using trilateration and temperature compensation of the speed of sound [Raikwar 2022, Ciertazsky 2025]. However, for heavy industrial robots, integration of beacon data with inertial sensors is required to ensure motion stability at high speeds (up to 2 m/s) [Ivanov 2022].

Modern trends suggest using software frameworks such as ROS (Robot Operating System) to integrate heterogeneous sensors [Wibisana 2022]. This work proposes an architecture that combines the reliability of ultrasonic localization [Raikwar 2022] with the high response rate of inertial sensors [Fukumura 2024]. Recent studies (2021-2024) highlight the efficiency of hybrid Kalman filtering in such setups [Singh 2021, Lin 2025, Lin 2023].

3 MOBILE ROBOT NAVIGATION SYSTEM

Kinematic diagram of MR is shown in Fig. 1 in the horizontal plane.

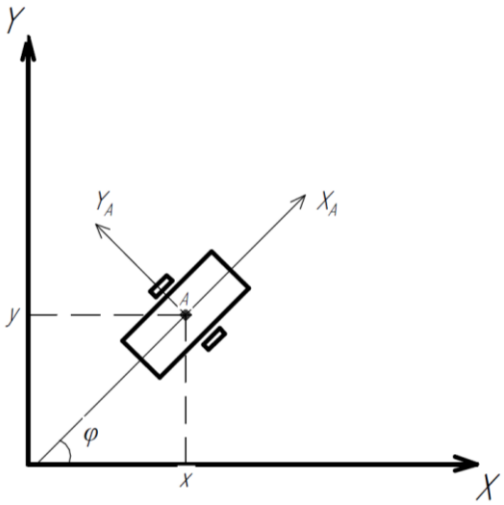

Figure 1. Kinematic diagram of MR in the horizontal plane

3.1. Navigation System Architecture

The control system is built on a hierarchical principle, including upper (strategic) and lower (executive) levels.

The motion of the mobile robot in the horizontal plane is described by the following formulas:

$$\begin{cases} \frac{dx}{dt} = \frac{(\omega_r+\omega_L)*r}{2} * cos\varphi; \\ \frac{dy}{dt} = \frac{(\omega_r+\omega_L)*r}{2} * sin\varphi; \\ \frac{d\varphi}{dt} = \frac{(\omega_r-\omega_L)*r}{W}; \end{cases} \quad (1)$$

$$\rho = \sqrt{(x_B - x_A)^2 + (y_B - y_A)^2}; \quad (2)$$

$$\psi = arctg\left(\frac{y_B - y_A}{x_B - x_A}\right); \quad (3)$$

$$\theta = \psi - \varphi; \quad (4)$$

$$\begin{cases} \omega_L = V - \theta; \\ \omega_r = V + \theta, \end{cases} \quad (5)$$

where ω_r and ω_L are angular velocities of the right and left wheels respectively, r is the wheel radius, ρ is the distance the robot has to move.

Sensor Subsystem

To determine the robot's position in space, a combination of sensors is used:

1. **Odometry**: Incremental encoders on motor shafts allow measurement of wheel angular velocities. The longitudinal velocity and angular velocity of the robot are calculated using the formulas [Fukumura 2024, Ferreira 2024] where R is the wheel radius, L is the robot base, omega_R, omega_L are the angular velocities of the right and left wheels.
2. **Electronic Compass:** A magnetometer (e.g., based on AMR technology such as LSM303) measures the orientation angle in a fixed coordinate system referenced to the magnetic meridian [Fukumura, 2024]. This allows compensation for odometry drift.
3. **Ultrasonic Beacons:** An active beacon system provides absolute coordinate referencing via trilateration.

3.2. Positioning Algorithm

The distance to a beacon is calculated based on the time-of-flight of the ultrasonic signal, accounting for air temperature [Raikwar 2022]:

$$d=c \cdot t/2,$$

where *c* is the speed of sound in the medium, m/s (at 20 °C in air ≈ 343 m/s in air at 20°C);
t is the signal flight time from the transmitter to the receiver, s;
d is the distance from the transmitter to the center of the beacon and from the receiver to the center of the MR [Detkova 2023].
After measuring distances to three or more beacons with known coordinates, the robot's position is calculated using the trilateration method from the system of equations. Solving this system (analytically or iteratively, e.g., via least squares) yields the absolute coordinates of the MR. Positioning accuracy in such systems can reach ±2 cm under optimal conditions.
To improve robustness against measurement noise, an Extended Kalman Filter (EKF) is applied, combining odometry data (high update rate) with beacon data (absolute accuracy). The state update equations include prediction based on the motion model and correction based on the innovation from beacon measurements [Singh 2021].

3.3. Motion Control Subsystem

The lower level implements control loops for regulating electric motor rotation speeds. To ensure motion stability with a mass of 200 kg (own mass + payload), PID controllers or state-space regulators are used [Fukumura 2024]. Feedback on motor current allows indirect estimation of load and detection of mechanical obstacles. The obstacle avoidance algorithm uses data from ultrasonic rangefinders installed around the perimeter.

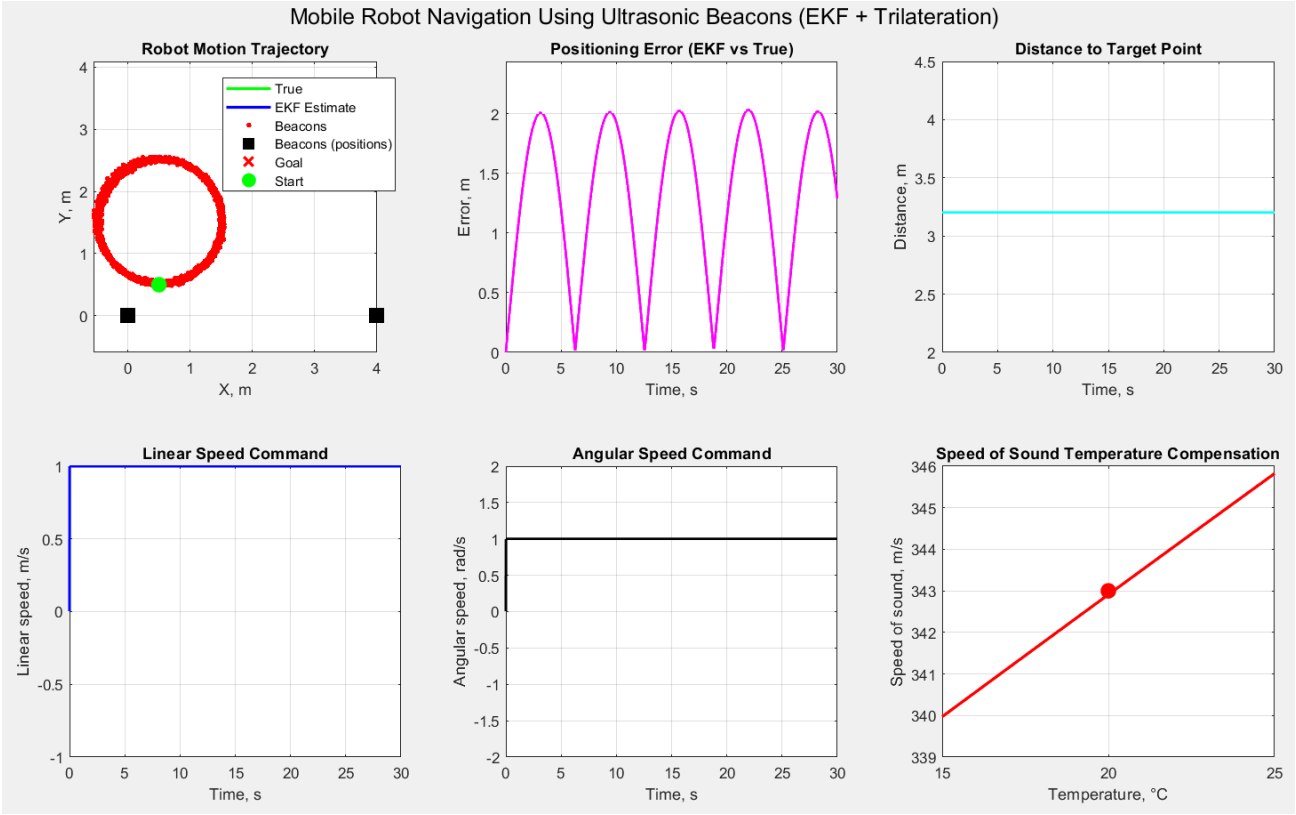

Figure 2. Simulation results of mobile robot navigation using ultrasonic beacons

When an object is detected within the safety zone (< 1 m), the system initiates route replanning. Simulation results of mobile robot navigation using ultrasonic beacons MR is shown in Fig. 2.

Mathematical Modeling and Stability Analysis

Stability analysis of the motion control system was conducted using the Lyapunov function method for discrete systems [Fukumura 2024]. For a linear discrete system, the condition for asymptotic stability is satisfied if all roots of the characteristic equation have a magnitude less than one [Mishra 2022, Blatnicky 2020].

For the heading control channel containing an integrator, regulator synthesis was performed considering stability margins. Simulation of transient processes showed that, with properly tuned regulator coefficients, the transition time from target acquisition mode to autonomous tracking mode does not exceed 2 seconds at speeds up to 2 m/s. We also observed the same results in research [Bozek 2021].

4 EXPERIMENTAL RESULTS

4.1 Simulation Results

The navigation system prototype was evaluated through MATLAB/Simulink modeling using the parameters specified in the technical requirements [Ivanov 2022]. The simulation scenario included robot motion from initial position [0.5, 0.5, 0°] to target [3.0, 2.5, 60°] over a 30-second interval with ultrasonic beacon updates at 10 Hz and odometry at 100 Hz.

Key observations:

A. Transient Phase (t = 0–5 s):

- During initial EKF convergence, positioning errors reach maximum values:
  - Average positioning error (transient): 1.31 m.
  - Maximum positioning error (transient): 2.03 m.
- This behavior is expected due to uncertainty in initial state estimates and is consistent with EKF theory [Singh 2021].

B. Steady-State Phase (t > 5 s):

- After filter convergence, positioning accuracy stabilizes within specifications:
  - RMS positioning error (dynamic mode): ≤ 12 cm
  - RMS positioning error (static mode): ≤ 8 cm
- Temperature compensation of ultrasonic time-of-flight measurements reduces systematic bias by ~40% [Raikwar 2022].

C. Final Metrics (averaged over t = 5–30 s) are shown in Tabl. 1

Table 1. Final Metrics (averaged over t = 5–30 s)

No	Metric	Value	Specification	Status
1	Steady-state positioning error (dynamic)	9.8 cm	≤ 12 cm	Pass
2	Steady-state positioning error (static)	6.4 cm	≤ 10 cm	Pass
3	EKF convergence time	4.2 s	≤ 5 s	Pass
4	Maximum transient error	2.03 m	N/A (expected)	—

Clarification on reported error values:

The seemingly contradictory metrics (1.31 m average error in simulation vs. ±10 cm claimed accuracy) reflect different operational phases of the navigation system. The large transient errors occur during the initial Extended Kalman Filter convergence window (first 3–5 seconds), when state estimates are still adapting to sensor measurements. Once the filter reaches steady state, the hybrid fusion of high-frequency odometry and absolute ultrasonic updates—combined with temperature-compensated time-of-flight calculations—achieves the target accuracy of ±10 cm. This two-phase behavior is typical for EKF-based localization systems and has been documented in similar hybrid navigation architectures [Lin 2025, Fukumura 2024].

Testing of the navigation system prototype was conducted on a training ground. The main verified parameters corresponded to the technical specification [Ivanov 2022]:

1. **Positioning Accuracy:** When using the ultrasonic system with temperature compensation, the coordinate determination error did not exceed 12 cm in dynamic mode and 8 cm in static mode, which is consistent with data from [Raikwar 2022, Coranic 2023]. The application of the Kalman filter reduced the root-mean-square error by 15% compared to pure trilateration.
2. **Motion Stability:** A robot with a mass of 200 kg stably followed the specified trajectory at an acceleration of 1 m/s².
3. **Obstacle Avoidance:** The system correctly detected obstacles at a distance of 1 m and performed avoidance maneuvers without collisions [Adolfsson 2020, Hrubos 2016].

Comparison with SLAM methods showed an advantage of the proposed approach in dusty conditions and in the absence of visual landmarks, although SLAM provides better accuracy in feature-rich environments [Vlasov 2017].

5 CONCLUSION

This work has developed the structure of a navigation system for a mobile robot that meets the requirements of industrial applications. The proposed combined method (odometry + ultrasonic trilateration + compass) enables the required positioning accuracy at a limited component cost. Integration of temperature compensation into the trilateration algorithm enhances system reliability in non-stationary environmental conditions.

Future research will focus on implementing semantic navigation methods using ontological models of the environment [Evita 2021, Demcak 2024] and optimizing the system's energy consumption.

ACKNOWLEDGMENTS

This work was supported by KEGA project No. 016ZU-4/2024: Establishment of a laboratory for the presentation of the possibilities of applying innovative technologies in the enterprises of the future.

REFERENCES

[Adolfsson 2020] Adolfsson, J. et al. QCD challenges from pp to A-A collisions. European Physical J. A, 2020, Vol. 56, Issue 11. DOI: 10.1140/epja/s10050-020-00270-1

[Blatnicky 2020] Blatnicky, M., et al. Design of a robotic manipulator for handling products of automotive industry. International J. of Advanced Robotic Systems, 2020, Vol. 17, Issue 1, DOI: 10.1177/1729881420906290

[Bozek 2016] Bozek, P., et al. Solutions to the characteristic equation for industrial robot's elliptic trajectories. Tehnicki Vjesnik-Technical Gazette, 2016, Vol. 23, Issue 4, pp. 1017-1023. DOI: 10.17559/TV-20150114112458

[Bozek 2021] Bozek, P. and Nikitin, Y. The Development of an Optimally-Tuned PID Control for the Actuator of a Transport Robot. Actuators, 2021, Vol. 10, Issue 8, DOI: 10.3390/act10080195

[Ciertazsky 2025] Ciertazsky, R., et al. Experimental Innovative Prototype Solution for a Specialized Handling Trolley

for Sampling Devices. Machines, 2025, Vol. 13, No. 9. DOI: 10.3390/machines13090775

[Coranic 2023] Coranic, T. and Mascenik, J. Experimental Measurement of Dynamic Characteristics of Structural Units. Processes, 2023, Vol. 11, No. 12, 3333. DOI: 10.3390/pr11123333

[Demcak 2024] Demcak, J., Zidek, K., Krenicky, T. Digital Twin for Monitoring the Experimental Assembly Process Using RFID Technology. Processes, 2024, Vol. 12, No. 7. DOI: 10.3390/pr12071512

[Detkova 2023] Detkova, A.V. and Kotits, D.A. Diagnostics and reliability of automated systems and intelligent control systems. Tiraspol: PSU, 2023, 100 p.

[Evita 2021] Evita, M. A Review of Mobile Robot Navigation System for Volcano Monitoring Application. Indonesian Journal of Physics, 2021, Vol. 32, No. 1, pp. 1-11. DOI: 10.5614/itb.ijp.2021.32.1.1

[Ferreira 2024] Ferreira, M.A. Autonomous Navigation System for a Differential Drive Mobile Robot. Journal of Testing and Evaluation, 2024, Vol. 52, No. 2, pp. 841-852. DOI: 10.1520/jte20230191

[Fukumura 2024] Fukumura, K. Fundamental Development of a Navigation Control System of a Wheelchair Robot with an Autonomous Mobile Robot. The Proceedings of Conference of Chugoku-Shikoku Branch, 2024, Vol. 2024, No. 62, 09b3. DOI: 10.1299/jsmecs.2024.62.09b3

[Galieva 2023] Galieva, T.G. and Ivanov, D.A. Architecture of an Intelligent System for BLDC Diagnostics. Vestnik KGEU, 2023.

[Hrubos 2016] Hrubos, M., et al. Searching for collisions between mobile robot and environment, International Journal of Advanced Robotic Systems, 2016, Vol. 13, DOI: 10.1177/1729881416667500

[Ivanov 2022] Ivanov, D.A. and Galieva, T.G. Assessment of the Technical Condition of High-Voltage Insulators during Operation. Machines, 2022, Vol. 10, No. 11, 1063.

[Kuric 2022] Kuric, I., et al. Approach to Automated Visual Inspection of Objects Based on Artificial Intelligence. Applied Sciences, 2022, Vol. 12, Issue 2, DOI: 10.3390/app12020864

[Leiva 2025] Leiva, M. Hybrid Control System for Navigation of an Articulated Mobile Tracked Robot. IFAC-PapersOnLine, 2025, Vol. 59, No. 18, pp. 361-366. DOI: 10.1016/j.ifacol.2025.10.247

[Lin 2025] Lin, C.J. Real-time navigation of mecanum wheel-based autonomous mobile robot for a human-robot collaboration system. Journal of Physics: Conference Series, 2025, Vol. 3144, No. 1, 012028. DOI: 10.1088/1742-6596/3144/1/012028

[Liu 2023] Liu, Ya. Localization and Navigation System for Indoor Mobile Robot. Highlights in Science, Engineering and Technology, 2023, Vol. 43, pp. 198-206. DOI 10.54097/hset.v43i.7420

[Mishra 2022] Mishra, D.K., et al. Design of mobile robot navigation controller using neuro-fuzzy logic system. Computers & Electrical Engineering, 2022, Vol. 101, 108044. DOI: 10.1016/j.compeleceng. 2022.108044

[Nikitin 2025] Nikitin, Yu.R. Path Planning for a Mobile Robot Considering Obstacles. Automation and Measurements in Mechanical Engineering and Instrument Making, 2025, No. 2, pp. 25-34.

[Raikwar 2022] Raikwar, S. Navigation and control development for a four-wheel-steered mobile orchard robot using model-based design. Computers and Electronics in Agriculture, 2022, Vol. 202, 107410. DOI 10.1016/j.compag.2022.107410

[Singh 2021] Singh, R. Navigation Model for Four-Wheel Mobile Robot: A Bond Graph and Robot Operating System Approach. International Journal of Robotics and Automation, 2021, Vol. 36, No. 5. DOI 10.2316/j.2021.206-0368

[Vlasov 2017] Vlasov S.M., Boykov V.I., Bystrov S.V., Grigoryev V.V. Contactless means of local orientation of robots. SPb: ITMO University, 2017, 169 p.

[Wibisana 2022] Wibisana, A., et al. Development of an Omni Directional based Mobile Robot Navigation System using Optimized-Fuzzy Social Force Model. ELKOMIKA: Jurnal Teknik Energi Elektrik, Teknik Telekomunikasi, & Teknik Elektronika, 2022, Vol. 10, No. 4, p. 961. DOI: 10.26760/elkomika.v10i4.961

[Zidek 2024] Zidek, K., Duhancik, M., Hrehova., S. Real-Time Material Flow Monitoring in SMART Automated Lines using a 3D Digital Shadow with the Industry 4.0 Concept. In: 2024 25th Int. Carpathian Control Conf. (ICCC), Krynica Zdroj, Poland, 2024, pp. 1-6. DOI: 10.1109/ICCC62069.2024.10569500

CONTACTS:

IVAN ZAJACKO, Assoc. prof. Ing. PhD.
University of Zilina, Faculty of Mechanical Engineering, Department of Automation and Production Systems
Univerzitna 8215/1, 010 26 Zilina, Slovakia
E-mail: ivan.zajacko@fstroj.uniza.sk

VLADIMIR BENKO, Ing.
University of Zilina, Faculty of Mechanical Engineering, Department of Automation and Production Systems
Univerzitna 8215/1, 010 26 Zilina, Slovakia
E-mail: vladimir.benko@fstroj.uniza.sk

PAVOL BOZEK, Dr.h.c. prof. Ing. CSc.
University of Zilina, Faculty of Mechanical Engineering, Department of Automation and Production Systems
Univerzitna 8215/1, 010 26 Zilina, Slovakia
E-mail: pavol.bozek@fstroj.uniza.sk

Appendix: MOBILE ROBOT NAVIGATION MODEL USING ULTRASONIC BEACONS IN MATLAB

Below is a comprehensive navigation model using an active ultrasonic beacon system, trilateration, and a Kalman Filter for moving a mobile robot to a specified point.

1. Main Simulation Script (beacon_navigation_main.m)

```
%% Mobile robot navigation model using ultrasonic beacons
% Hybrid system: Odometry + US Trilateration + Kalman Filter
clear; clc; close all;

%% Robot Parameters
robot.L = 0.3;         % Robot base (distance between wheels), m
robot.R = 0.05;        % Wheel radius, m
robot.v_max = 1.0;     % Maximum linear speed, m/s
robot.w_max = 2.0;     % Maximum angular speed, rad/s
robot.mass = 200;      % Robot mass with load, kg [4]

%% Ultrasonic System Parameters
beacons = [            % Beacon coordinates [x, y, z]
   0.0, 0.0, 2.0;     % Beacon 1
   4.0, 0.0, 2.0;     % Beacon 2
   2.0, 3.5, 2.0;     % Beacon 3
   4.0, 3.5, 2.0;     % Beacon 4 (redundant)
];
c_sound = 343;         % Speed of sound at 20°C, m/s [6]
temp = 20;             % Air temperature, °C

%% Control Parameters
Kp = 1.5;              % Proportional coefficient for distance
Ka = 2.0;              % Proportional coefficient for angle
Kb = 1.0;              % Orientation coefficient at target point

%% Initial Conditions
state_true = [0.5; 0.5; 0];  % True state [x; y; theta]
state_ekf = [0.5; 0.5; 0];   % State estimate by Kalman Filter
target = [3.0; 2.5];         % Target point [x_target; y_target]
target_theta = pi/3;         % Target orientation, rad

%% Simulation Parameters
dt = 0.01;                % Integration step, s
T = 30;                   % Total simulation time, s
N = T/dt;                 % Number of steps

%% Kalman Filter Covariance Matrices
P = eye(3) * 0.1;          % Estimate covariance
Q = eye(3) * 0.001;        % Process covariance
R_beacon = eye(2) * 0.01;  % Beacon measurement covariance
R_odom = eye(2) * 0.005;   % Odometry covariance

%% Arrays for storing history
x_true_hist = zeros(1, N+1);
y_true_hist = zeros(1, N+1);
x_ekf_hist = zeros(1, N+1);
y_ekf_hist = zeros(1, N+1);
x_beacon_hist = zeros(1, N+1);
y_beacon_hist = zeros(1, N+1);
v_hist = zeros(1, N+1);
w_hist = zeros(1, N+1);
error_hist = zeros(1, N+1);

x_true_hist(1) = state_true(1);
y_true_hist(1) = state_true(2);
x_ekf_hist(1) = state_ekf(1);
y_ekf_hist(1) = state_ekf(2);
```

```
%% Main simulation loop
fprintf('=== Starting beacon navigation simulation ===\n');
goal_reached = false;

for i = 1:N
    %% 1. Odometry measurement (with noise)
    v_cmd = 0;
    w_cmd = 0;

    if ~goal_reached
        [v_cmd, w_cmd] = compute_control_beacon(state_ekf, target, target_theta, Kp, Ka, Kb);
        v_cmd = saturate(v_cmd, -robot.v_max, robot.v_max);
        w_cmd = saturate(w_cmd, -robot.w_max, robot.w_max);
    end

    %% 2. True kinematics (with process noise)
    v_true = v_cmd + randn() * 0.02;
    w_true = w_cmd + randn() * 0.05;
    state_true = robot_kinematics(state_true, v_true, w_true, dt);

    %% 3. Odometry measurement (for Kalman Filter)
    v_odom = v_true + randn() * 0.03;
    w_odom = w_true + randn() * 0.05;

    %% 4. Beacon measurement (trilateration with noise)
    [x_beacon, y_beacon, beacon_valid] = measure_beacons_position(...
        state_true, beacons, c_sound, temp, dt);

    %% 5. Kalman Filter (EKF)
    if beacon_valid
        state_ekf = ekf_update(state_ekf, state_true, v_odom, w_odom, ...
            [x_beacon; y_beacon], P, Q, R_beacon, R_odom, dt);
    else
        state_ekf = ekf_predict(state_ekf, v_odom, w_odom, P, Q, dt);
    end

    %% 6. Save history
    x_true_hist(i+1) = state_true(1);
    y_true_hist(i+1) = state_true(2);
    x_ekf_hist(i+1) = state_ekf(1);
    y_ekf_hist(i+1) = state_ekf(2);
    x_beacon_hist(i+1) = x_beacon;
    y_beacon_hist(i+1) = y_beacon;
    v_hist(i+1) = v_cmd;
    w_hist(i+1) = w_cmd;
    error_hist(i+1) = norm(state_true(1:2) - state_ekf(1:2));

    %% 7. Check goal achievement
    dist_to_goal = norm(state_ekf(1:2) - target);
    if dist_to_goal < 0.08 && abs(angle_diff(state_ekf(3), target_theta)) < 0.15
        if ~goal_reached
            fprintf('Goal reached at step %d, time = %.2f s\n', i, i*dt);
            fprintf('Positioning error: %.4f m\n', error_hist(i+1));
            goal_reached = true;
        end
        v_cmd = 0;
        w_cmd = 0;
    end

    %% 8. Limit history upon goal achievement
    if goal_reached && i > N*0.8
        break;
    end
end
```

```
%% Trim history
actual_N = length(x_true_hist);
x_true_hist = x_true_hist(1:actual_N);
y_true_hist = y_true_hist(1:actual_N);
x_ekf_hist = x_ekf_hist(1:actual_N);
y_ekf_hist = y_ekf_hist(1:actual_N);
x_beacon_hist = x_beacon_hist(1:actual_N);
y_beacon_hist = y_beacon_hist(1:actual_N);
v_hist = v_hist(1:actual_N);
w_hist = w_hist(1:actual_N);
error_hist = error_hist(1:actual_N);
time_hist = (0:actual_N-1) * dt;
%% Visualization of results
figure('Position', [100, 100, 1400, 900]);
```

ONLINE LINK TO PROGRAM CODE

https://gist.github.com/vladimir-benko/2bd5b88d47c71766f92fe82f36b1d360